INL/CON-24-76493-Revision-0

Experimental and Analytical Verification of ASME Section IiII Division 5 Creep-Fatigue Design Rules

November 2024

Yanli Wang, R. I. Jetter, Ting-Leung Sham

Changing the World's Energy Future

INL is a U.S. Department of Energy National Laboratory operated by Battelle Energy Alliance, LLC

INL/CON-24-76493-Revision-0

Experimental and Analytical Verification of ASME Section IIII Division 5 Creep-Fatigue Design Rules

Yanli Wang, R. I. Jetter, Ting-Leung Sham

November 2024

Idaho National Laboratory
Idaho Falls, Idaho 83415

http://www.inl.gov

Prepared for the
U.S. Department of Energy
Under DOE Idaho Operations Office
Contract DE-AC07-05ID14517

Proceedings of the ASME 2024
Pressure Vessels & Piping Conference
PVP2024
July 28-August 2, 2024, Bellevue, Washington

PVP2024-123351

EXPERIMENTAL AND ANALYTICAL VERIFICATION OF ASME SECTION III, DIVISION 5 CREEP-FATIGUE DESIGN RULES

Yanli Wang[1], Robert Jetter[2], and Ting-Leung Sham[3]

[1]Oak Ridge National Laboratory, Oak Ridge, Tennessee, USA
[2]R. I. Jetter Consulting, Pleasanton, California, USA
[3]Idaho National Laboratory, Idaho Falls, Idaho, USA

ABSTRACT

The continuous advancement of structural materials and the growing demands for more reliable and economical structural components in high-temperature reactor applications have necessitated the development of comprehensive design methodologies and design rules. Mechanical degradation of structural components at elevated temperatures subjected to cyclic deformation is controlled by the creep-fatigue damage. Over the past few decades, diligent research efforts have been dedicated to refining the development of elevated temperature design rules in the American Society of Mechanical Engineers (ASME) Boiler and Pressure Vessel Code (BPVC), Section III, Division 5 and to develop conservative design rules that can effectively guard against the risk of creep-fatigue failure.

In ASME Section III, Division 5, for a design to pass the creep-fatigue acceptance criteria, creep damage and fatigue damage are evaluated separately, and these damages must not violate the bi-linear creep-fatigue interaction diagram, i.e., the so-called D-diagram. The creep-fatigue damage evaluation procedure assumes that the effects of the actual cyclic loading sequence can be bounded by assuming that the individual loading cycles are uniformly distributed throughout the component design life. In this study, creep-fatigue experiments with variable amplitudes and loading sequencies were designed and performed on Alloy 617 at high temperatures. The results were analyzed to evaluate the loading history effect on creep-fatigue damage accumulation and to verify the assumptions for the creep-fatigue evaluation design rules.

Keywords: Creep-fatigue, damage summation

NOMENCLATURE

i	cycle number i
N	number of cycles
d_c^i	creep damage fraction of cycle i based on time fraction
D_{cf}	creep-fatigue damage fraction
D_f	fatigue damage fraction
σ	stress
ϵ	strain
N_f	average failure cycles of pure fatigue testing
N_{cf}	average failure cycles of creep-fatigue tests under the same condition.
w^i	dissipated work in the stress-strain hysteresis loop of cycle i
w_f	accumulated dissipated work in the stress-strain hysteresis loop upon failure

1. INTRODUCTION

Creep-fatigue (CF) interactive damage represents the most significant degradation mechanism for structural components operating under cyclic loads at elevated temperatures. Over the past few decades, extensive research efforts have been devoted to refining the development of elevated temperature design rules within the American Society of Mechanical Engineers (ASME) Boiler and Pressure Vessel Code (BPVC), Section III, Division 5 [1], aiming to establish conservative design rules capable of effectively mitigating the risk of creep-fatigue failure.

The current Subsection HB, Subpart B CF evaluation method in the design procedure relies on the damage-diagram (or D-diagram), which requires separate assessments of fatigue damage and creep damage. A design passes the CF check if the evaluation demonstrates that the accumulated creep damage and fatigue damage fall within the bilinear envelope in the D-diagram.

Recently, an alternative CF evaluation approach based on the simplified model test (SMT) design methodology has been under development [2]. This approach aims to simplify the CF evaluation procedure and minimize the over-conservatism

inherent in the current ASME D-diagram approach, while adequately accounting for enhanced creep damage at localized defects and stress risers [3, 4]. In this method, the accumulated CF damage is also assumed to be a linear summation of the CF damage from all different cycle types.

In practice, the sequence of CF cycle types throughout the design lifetime is often unknown. Both aforementioned approaches assume a uniform distribution of different CF cycle types throughout the design lifetime, with the final CF evaluation check through a linear summation of all CF cycle types during the entire design life. The influence of the sequence of different cycle types is not considered. In this study, experiments were designed to evaluate these assumptions using Alloy 617 on standard lab-scale specimens. The testing temperature was set at 850°C, where Alloy 617 is in the creep regime, and there is a considerable amount of stress relaxation during strain-controlled CF loading.

2. EXPERIMENTAL AND ANALYSIS METHODS

2.1 Material and experimental

The solution annealed hot-rolled Alloy 617 plate with Heat number 314626 from ThyssenKrupp VDM USA Inc. was used to fabricate test specimens for this study. The material plate has a nominal thickness of 38 mm. Table 1 lists the chemical compositions of the Alloy 617 plate. The Alloy 617 plate in this study is one of the heats of material utilized in producing the data package for ASME Section III Division 5 Alloy 617 Code Cases N-898 and N-872.

TABLE 1. CHEMICAL COMPOSITIONS OF THE ALLOY 617 PLATE WITH HEAT NUMBER 314626 (WT%)

C	S	Cr	Mn	Si	Mo	Ti
0.05	<0.002	22.2	0.1	0.1	8.6	0.4
Cu	**Fe**	**Al**	**Co**	**B**	**Ni**	
0.04	1.6	1.1	11.6	<0.001	balance	

Standard creep-fatigue specimen geometry shown in Figure 1 was used in this study. The specimen gage section was prepared with low stress grinding process and polished to #8 surface finish.

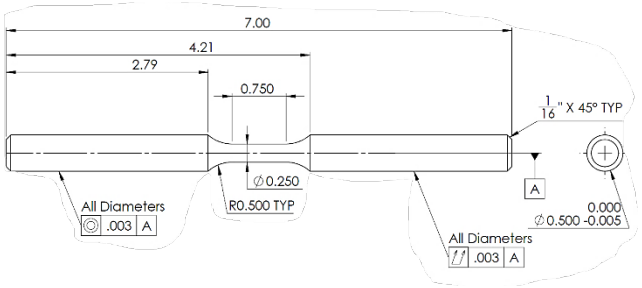

FIGURE 1. CREEP-FATIGUE SPECIMEN GEOMETRY. DIMENSIONS ARE IN INCHES.

The CF testing was under strain-controlled mode with the straining profile schematically shown in Figure 2. The hold-time segment was applied to the maximum tension-strain amplitude, maximum compression amplitude or both tension and compression peak amplitude for creep-fatigue loading. The straining profile is a fully reversed profile (i.e., with a nominal straining ratio of $R = -1$). The nominal strain rate is 1×10^{-3}/s.

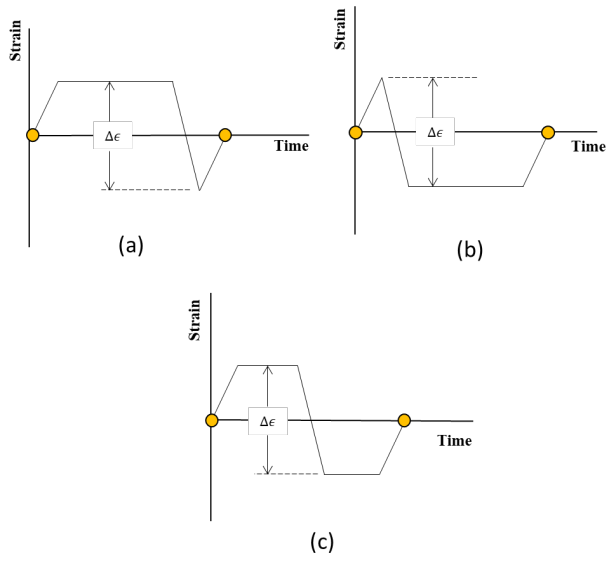

FIGURE 2. STRAIN-CONTROLLED CREEP-FATIGUE STRAINING PROFILE FOR ONE CYCLE WITH (A) TENSION HOLD, (B) COMPRESSION HOLD, AND (C) COMBINED TENSION AND COMPRESSION HOLD.

2.2 Creep-fatigue damage analysis methods

Energy-based damage analysis

In this study, the CF damage at cycle i, w^i, is assessed by the dissipated work:

$$w^i = \int \sigma d\epsilon \tag{1}$$

where σ is the stress and ϵ is the strain. And the dissipated work accumulated at failure cycle, w_f, is given by:

$$w_f = \sum_{1}^{N_{cf}} w^i \tag{2}$$

where N_{cf} is the number of cycles to failure for the CF testing. For simplification, the w_f is often estimated using the mid-life cycle damage w^{mid}, using $w_f = w^{mid} \times N_{cf}$. Our detailed analysis showed little difference in the w_f calculation results for Alloy 617 at 850 °C and 950 °C. The reason is that the CF deformation behavior for Alloy 617 is stable throughout the CF

life, and a subset of the cycles or mid-life cycle could reasonably represent the overall CF deformation behavior.

Time fraction based creep damage evaluation

The CF evaluation procedure in Section III, Division 5 of the ASME Boiler and Pressure Vessel Code uses time fraction method for creep damage evaluation. The creep damage at cycle i, d_c^i, is calculated by:

$$d_c^i = \int_0^{t_h} \frac{1}{t_f(\sigma,T)} dt \tag{3}$$

where $t_f(\sigma,T)$ is the creep rupture time. In this method, the average Alloy 617 creep rupture life is used, with the stress and temperature correlated in the form of a Larson-Miller relationship. The Larson-Miller relationship for Alloy 617 is give in reference [5]. The total creep damage, D_c, at failure is the summation of the creep damage from each cycle.

$$D_c = \sum_1^{N_{cf}} d_c^i \tag{4}$$

Similarly, the total creep damage is often estimated using the mid-life cycle creep damage d^{mid}, using $D_c = d^{mid} \times N_{cf}$ or based on a certain subset number of cycles. These approaches were demonstrated to show negligible difference in the creep damage calculation results for Alloy 617 at 850 ºC and 950 ºC [5].

Fatigue damage and creep-fatigue fraction

In this study, the fatigue-damage fraction for cycle type k, D_f^k, is defined as the ratio of the applied CF cycles, N^k, to the average failure cycles of the pure fatigue tests conducted under the same strain range, strain rate, and temperature, N_f^k.

$$D_f^k = \frac{N^k}{N_f^k} \tag{6}$$

Similarly, the CF damage for cycle type k, D_{cf}^k, is defined as the ratio of the applied CF cycles, N^k, to the failure cycles of those CF tests under the same condition.

$$D_{cf}^k = \frac{N^k}{N_{cf}^k} \tag{7}$$

Note that the average cycles to failure from duplicate tests are used to calculate the fatigue-damage and CF fraction, although there are very limited number duplicates generated.

When multiple-cycle types were applied, the total damage is a simple linear summation of corresponding damage from all cycle types.

3. RESULTS AND DISCUSSION

3.1 Standard CF on Alloy 617 at 850 ºC

In this study, standard CF tests were conducted using continuous strain-controlled cycling with a single straining profile. At a nominal strain range of 0.3%, three types of CF tests were performed: test T1 with a tensile hold of 600 seconds, test C1 with a compression hold of 600 seconds, and test TC1 combining a tension hold of 300 seconds and a compression hold of 300 seconds. The results from this study, along with those from reference [5], are summarized in Table 2. Although the data are limited, the general trend indicates that CF with tension hold is most damaging to Alloy 617 at 850°C, showing the lowest average cycles to failure, while CF loading with compression hold is least damaging to the material.

The results of CF at a 1% strain range with a tensile hold of 600 seconds, as well as the pure fatigue test results at strain ranges of 0.3% and 1% [5], are also summarized in Table 2.

TABLE 2. STANDARD CF TESTING ON 617 AT 850 ºC

Test No.	Nominal Strain range,	Tensile hold time, sec	Compression hold time, sec	Number of Cycles to failure
T1	0.3%	600	0	1774 ± 251 (4 tests)[1)]
TC1	0.3%	300	300	2285 (one test)
C1	0.3%	0	600	3093 (one test)
T2	1%	600	0	374± 172 (4 tests)[2)]
Pure fatigue[3)]	0.3%	0	0	110010
	1%	0	0	828

Note: 1) Three of the tests are from [5]. The 4th test from this study showed consistent results.
2) Two of the tests are from [5]. The cycles to failure were about twice of results from this study, resulting large data scatter.
3) The average cycles to failure of pure fatigue tests are from [5].

The midlife hysteresis loops of tests T1, TC1, and C1 are plotted in Figure 3. The total dissipated work of TC1 for this cycle, represented by the area of the hysteresis loop, almost encompasses both T1 and C1. Interestingly, the larger dissipated work for TC1 did not result in greater damage to the material or shorter CF life cycles.

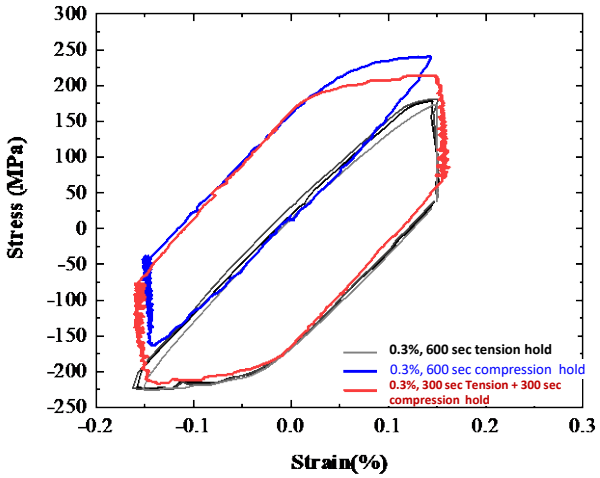

FIGURE 3. MID-LIFE HYSTERESIS LOOPS OF STANDARD CF TEST T1, TC1 AND C1

3.2 Multi-cycle type CF on Alloy 617 at 850 °C

In this section, five CF tests with multi-cycle types in the straining profile were designed and performed on Alloy 617 at 850 °C. Two cycle types were considered: one with a 1% strain and a 600-second tension hold, and the other with a 0.3% low strain range, also with a 600-second tension hold. The details of these tests are outlined below:

- Test **M1** has two segments: CF damage at 1% for 251 cycles followed by CF at 0.33% for 551 cycles to failure.
- Test **M2** has two segments: CF damage at 0.33% for 1600 cycles followed by CF at 1% for 35 cycles to failure.
- Test **M3** has two segments: CF damage at 0.33% for 824 cycles followed by CF at 1 % for 190 cycles to failure.
- Test **M4** has two segments**:** CF damage at 1% for 100 cycles followed by CF at 0.33% for 1344 cycles to failure.
- Test **M5** utilized a composite cycle for cycling. Each composite cycle unit consisted of 16 cycles at an average 0.18% strain range followed by 5 cycles at 1.16% strain range. The composite cycle unit was repeated till failure occurred.

The results are summarized in Table 3. The number of failure cycles was determined as the cycle at which there was a 20% drop in the ratio of the maximum stress to minimum stress as a function of applied cycles.

The maximum and minimum stresses as a function of the applied cycles for M1, M2, M3 and M4 are presented in Figures 4, 5, 6 and 7 respectively. The CF fraction was calculated for the two segments of M1, M2, M3, and M4 using the sum of the CF fraction, D_{cf}^{k}, value for each cycle type, where D_{cf}^{k} represents the ratio of the number of applied cycles for each cycle type to the average cycles to failure of the corresponding CF under the same loading condition.

The number of cycles to failure for test T1 at a 1% strain range, and that of test T2 at a 0.3% strain range listed in Table 2 were used for the calculation. For example, test M1 had the first segment at 1% for 251 cycles, which would result in a CF fraction of $(^{251}/_{374})$, i.e., 67%, and the second segment at 0.33% had a CF fraction of $(^{551}/_{1774})$ or 31%. The total CF fraction of 98% is the linear sum of the 67% and 31%. The same approach was used to calculate the CF fraction for M2, M3 and M4.

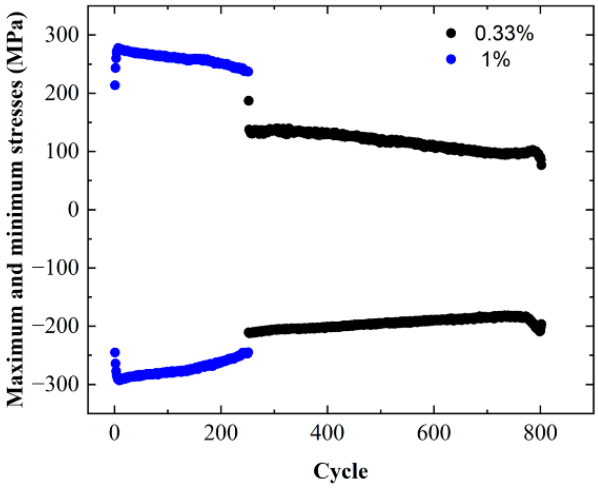

FIGURE 4. MAXIMUM AND MINIMUM STRESSES OF TEST M1

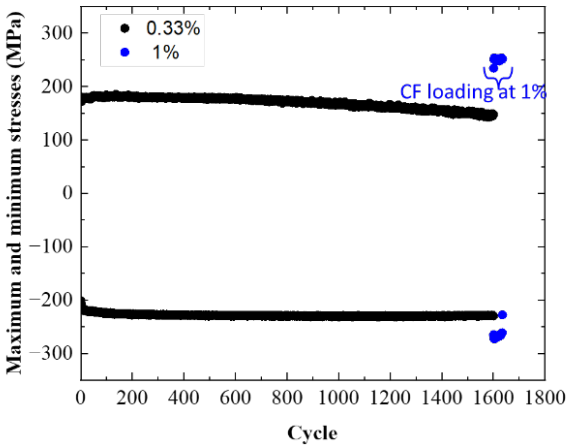

FIGURE 5. MAXIMUM AND MINIMUM STRESSES OF TEST M2

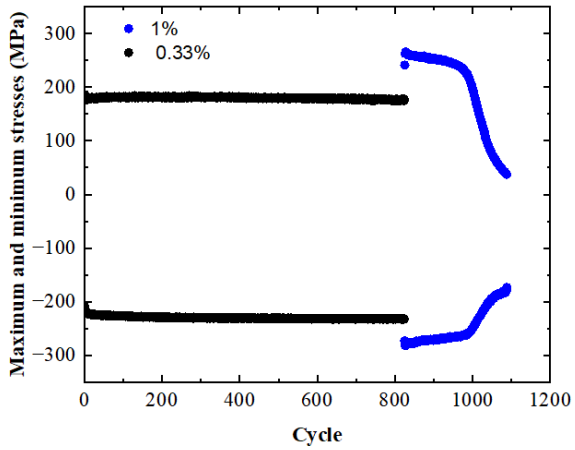

FIGURE 6. MAXIMUM AND MINIMUM STRESSES OF TEST M3

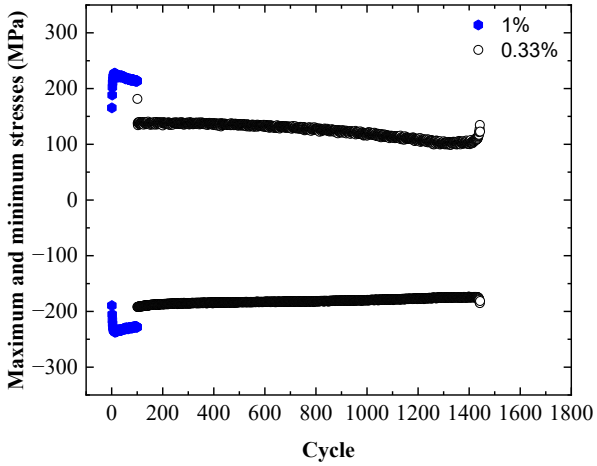

FIGURE 7. MAXIMUM AND MINIMUM STRESSES OF TEST M4

It is noted that test M5 had the most complex straining profile, involving intermittent switching between high and low strain ranges. However, the strain amplitude was not well controlled, showing an average of 0.18% for the low strain range instead of the target 0.3%. Figures 4 and 5 present the maximum stresses and the hysteresis loops of the initial composite cycles for M5.

In literature, there is a lack of experimental CF failure data at 0.18% with 600 sec tension hold time. However, in a recent analysis in [6], estimations suggest that the cycles to failure for CF are approximately 10,000 cycles at this strain range. Therefore, the total CF fraction at 0.18% is approximately 12%. On the other hand, the accumulated CF cycles at 1% strain range were 375, contributing to 100% of the CF fraction. The test results from M5 indicate that the addition of low strain range cycles in each composite cycle unit did not significantly affect the life of CF at a large strain range of 1%.

It is intriguing to observe that all five multi-cycle type tests exhibited total CF fractions within 100±10%, despite significant variations in strain profile, straining sequence, and the applied CF damage fraction at the initial segment.

TABLE 3. MULTI-CYCLE TYPE CF ON ALLOY 617 AT 850 ^{O}C

Test No.	Strain range and number of cycles for each segment	CF fraction, D_{cf}^{k}
M1	Seg.1. 1% for 251 cycles Seg.2. 0.33% for 551 cycles to failure	Seg.1. ~67% Seg.2. ~31% **Total: 98%**
M2	Seg.1. 0.33% for 1600 cycles Seg.2. 1% for 35 cycles to failure	Seg.1. ~90% Seg.2. ~9% **Total: 99%**
M3	Seg.1. 0.33% for 824 cycles Seg.2. 1% for 190 cycles to failure	Seg.1. ~46% Seg.2. ~50% **Total: 96%**
M4	Seg.1. 1% for 100 cycles Seg.2. 0.34% for 1344 cycles to failure	Seg.1. ~26% Seg.2. ~76% **Total: 102%**
M5	• 75 Composite cycle with (16 cycles at 0.2% followed by 5 cycles at 1.16%) • additional 16 cycles at 0.2% to failure	• 75 x (0.16%+1.3%) • additional 0.16% **Total: ~110%**

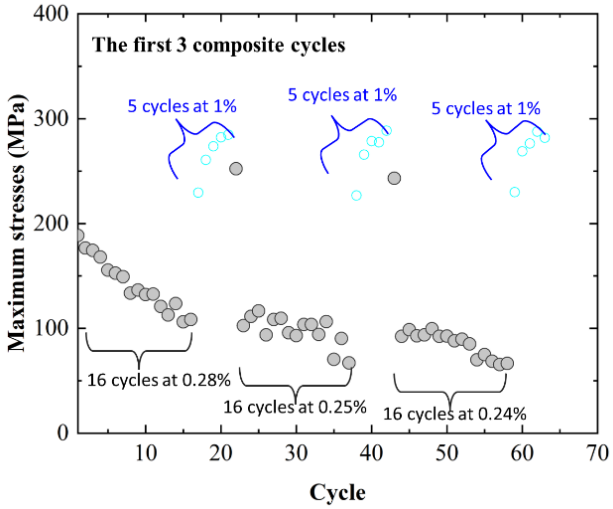

FIGURE 8. THE MAXIMUM STRESSES OF THE FIRST 3 COMPOSITE CYCLE UNITS OF TEST M5

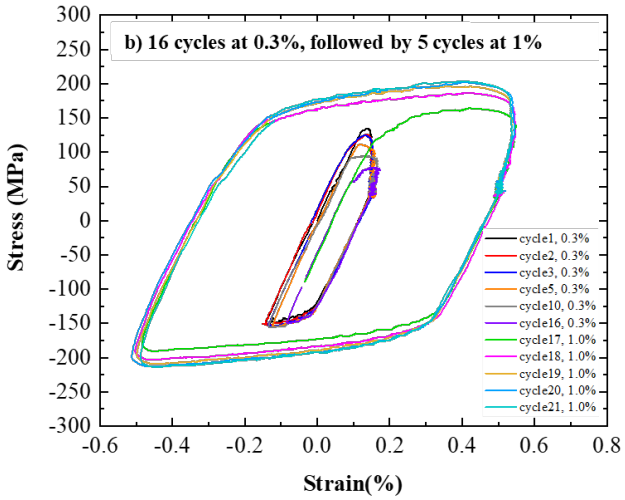

FIGURE 9. THE HYSTERYSIS LOOPS OF THE FIRST COMPOSITE CYCLE UNIT OF TEST M5

3.3 Discussions

The accumulated dissipated work of the CF tests was computed, and the results are summarized in Figure 10. It's important to note that the error bars for tests T1 and T2 are based on 4 tests each condition. TC1 exhibited the largest accumulated dissipated work upon failure, attributable to its high dissipated work per cycle, as depicted in Figure 3. The high accumulated dissipated work for C1 is due to its high number of cycles to failure.

In standard CF tests with the same tension hold time of 600 seconds, there is no clear evidence of strain range dependence based on the available data, likely due to significant data scatter. The multi-cycle type CF tests M1, M2, M3, M4, and M5 showed accumulated dissipated work values comparable to the standard test with tension hold.

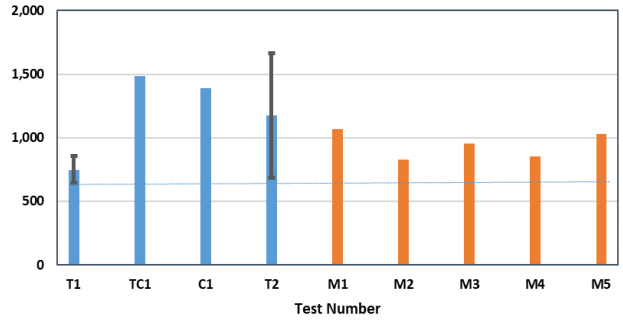

FIGURE 10. ACCUMULATED DISSIPATED WORK OF THE STANDARD AND MULIT-CYCLE TYPE CF ON ALLOY 617 AT 850 ^{O}C

The multi-cycle type CF tests M1, M2, M3, M4 and M5 were analyzed for their total creep damage Dc based on time-fraction approach, and the total fatigue damage D_f. The results are plotted on the bi-linear D-diagram chart in Figure 11. The interception point of the bilinear envelope is [0.1, 0.1] for Alloy 617. The results from standard 850°C CF tests with tensile holds of 180 seconds, 600 seconds, 1800 seconds, and 3600 seconds at a 0.3% strain range, and those with tension holds of 180 seconds, 600 seconds, 1800 seconds, 3600 seconds, 7200 seconds, and 14400 seconds at a 1% strain range [5] are also presented and plotted.

The overall trend suggests that the accumulated creep damage at the 0.3% strain range is higher than that at 1%, but lower in accumulated fatigue damage. Additionally, increasing the applied hold time at both strain ranges results in a reduction in fatigue cycles. Notably, when the same hold time is applied, the decrease in cyclic life is more pronounced at the lower strain range of 0.3%. However, the multi-cycle type CF tests in this study blend in nicely with the standard CF tests with tension hold at these two strain ranges, without significant abnormality.

Based on this analysis, it is reasonable to conclude that the distribution of different cycle types in a design problem does not significantly affect the CF damage analysis results at elevated temperatures.

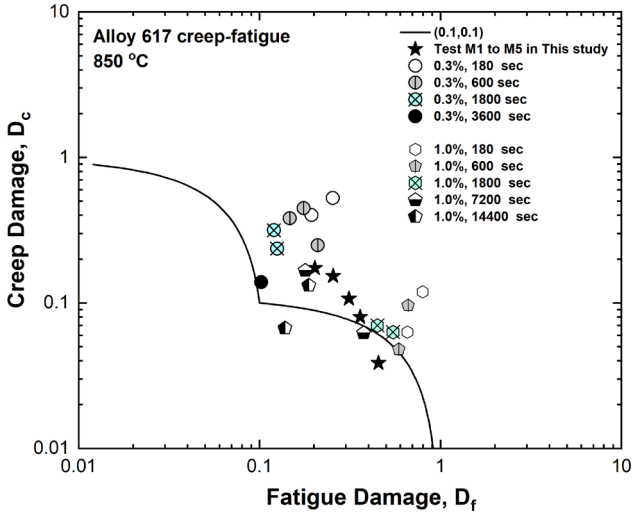

FIGURE 11. THE STANDARD [5] AND MULIT-CYCLE TYPE CF TEST RESTULS ON ALLOY 617 AT 850 ^{O}C ON D-DIAGRAM.

4. CONCLUSION

From this study, it can be concluded that CF testing with tension hold time at elevated temperatures is the most damaging to Alloy 617 compared to compression hold or combined tension and compression hold at the same strain range.

Additionally, the distribution of different cycle types in a design problem does not significantly affect the CF damage analysis results at elevated temperatures.

COPYRIGHT NOTICE

ACKNOWLEDGMENTS

The research was sponsored by the U.S. Department of Energy, Office of Nuclear Energy, under contract No. DE-AC05-00OR22725 with Oak Ridge National Laboratory (ORNL), managed and operated by UT-Battelle, LLC, and under contract No. DE-AC07-05ID14517 with Idaho National Laboratory (INL), managed and operated by Battelle Energy Alliance, LLC. Programmatic direction was provided by the Office of Nuclear Reactor Deployment of the Office of Nuclear Energy.

The contribution of Brad Hall and Charles S. Hawkins of ORNL in running the experiments is greatly appreciated. The authors acknowledge Peijun Hou of Imtech Corporation, Knoxville, Tennessee for the data analysis and technical support.

REFERENCES

[1] ASME Code Section III Rules for Construction of Nuclear Facility Components High Temperature Reactors, Division 5 High Temperature Reactors. 2023 edition, American Society of Mechanical Engineers.

[2] Wang, Y., Jetter, R. I., Messner, M., and Sham, T.-L. (2019), “Development of Simplified Model Test Method for Creep-fatigue Evaluation”, Proceedings of the ASME 2019 Pressure Vessels and Piping Conference, PVP2019-93648, American Society of Mechanical Engineers, New York, NY.

[3] Wang, Y., Jetter, R. I. and Sham, T.-L (2014), “Application of Combined Sustained and Cyclic Loading Test Results to Alloy 617 Elevated Temperature Design Criteria”, ORNL/TM-2014/294, Oak Ridge National Laboratory, Oak Ridge, TN.

[4] Wang, Y., Jetter, R. I., Messner, M., Mohanty, S., and Sham, T.-L. (2017), “Combined Load and Displacement Controlled Testing to Support Development of Simplified Component Design Rules for Elevated Temperature Service”, Proceedings of the ASME 2017 Pressure Vessels and Piping Conference, PVP2017-65455, American Society of Mechanical Engineers, New York, NY.

[5] Wright, R.N., Draft ASME Boiler and Pressure Vessel Code Cases and Technical Bases for Use of Alloy 617 for Construction of Nuclear Components Under Section Ill, Division 5, INL/EXT-15-36305, Revision 2, Idaho National Laboratory, Idaho Falls, Idaho.

[6] Wang, Y., Hou, P. and Sham, T.-L., An Extrapolation Method for Strain Ranges and Hold Times in Developing the EPP+SMT Creep-Fatigue Design Curves for Alloy 617, ORNL/TM-2022/ 2517, Oak Ridge National Laboratory, Oak Ridge, Tennessee.